The Role of Potassium Channels in the Temperature Control of Stomatal Aperture[1]

Nitza Ilan, Nava Moran, and Amnon Schwartz*

Department of Agricultural Botany, Faculty of Agriculture, The Hebrew University of Jerusalem, Rehovot 76100, Israel (N.I., A.S.); and Department of Neurobiology, Weizmann Institute, Rehovot 76100, Israel (N.M.)

We used the patch-clamp technique to examine the effect of temperature (13–36°C) on the depolarization-activated K channels (K_D channels) and on the hyperpolarization-activated channels (K_H channels) in the plasma membrane of *Vicia faba* guard-cell protoplasts. The steady-state whole-cell conductance of both K channel types increased with temperature up to 20°C. However, whereas the whole-cell conductance of the K_H channels increased further and saturated at 28°C, that of K_D channels decreased at higher temperatures. The unitary conductance of both channel types increased with temperature like the rate of diffusion in water (temperature quotient of approximately 1.5), constituting the major contribution to the conductance increase in the whole cells. The mean number of available K_H channels was not affected significantly by temperature, but the mean number of available K_D channels increased significantly between 13 and 20°C and declined drastically above 20°C. This decrease and the reduced steady-state voltage-dependent probability of opening of the K_D channels above 28°C (because of a shift of voltage dependence by +21 mV) account for the depression of the whole-cell K_D conductance at the higher temperatures. This may be a basic mechanism by which leaves of well-watered plants keep their stomata open during heat stress to promote cooling by transpiration.

Diffusion of both water vapor and CO_2 across the leaf epidermal tissue is modulated by variation in stomatal aperture. In the intact leaf as well as in isolated epidermal strips, the aperture of the stomatal pore is controlled by diverse environmental signals, such as light, humidity, CO_2 concentration, and temperature (Zeiger, 1983; Mansfield et al., 1990; Assmann, 1993). When the leaf temperature increases, stomata tend to open wider in unstressed plants of a number of C_3 and C_4 species (Raschke, 1975; Sheriff, 1979; Berry and Bjorkman, 1980, and refs. therein). In leaves of a well-watered plant at high temperature, large stomatal conductance will promote transpirational cooling and thereby will keep the leaf temperature lower than that of the surrounding air (Gates, 1968; Radin et al., 1994).

Simultaneous measurements of photosynthesis and stomatal conductance in well-watered *Zea mays* (Raschke, 1970) and *Eragrostis tef* (Kebede et al., 1989) leaves, exposed to heat-stress conditions (>40°C), indicated that stomatal conductance remained high even when photosynthesis was temporarily impaired. Furthermore, down-regulation of leaf temperature in extreme heat conditions will be more efficient if stomata closing signals are ignored. Indeed, at high temperature (>35°C) open stomata of *Z. mays* became insensitive to the increase in the leaf internal CO_2 concentration, a known signal for stomatal closing. In intact leaves of *Xanthium pennsylvanicum* that were exposed to high temperature (36°C), stomata opened even in the dark. The dark opening was then followed by a slow reclosure. The rate of stomatal closure in the dark was significantly slower at a high (36°C) than at a lower (27°C) temperature (Mansfield, 1965). Similarly, in intact leaves of *Vicia faba* (Kappen et al., 1994) and in isolated epidermal strips of the same species (Rogers et al., 1979, 1981) stomata opened wider at high temperature (>28°C) and stayed open even in darkness.

Stomatal opening occurs by increasing the turgor pressure of guard cells, which is achieved by osmotic water influx following the increase in the concentrations of K^+, Cl^-, and organic solutes in the cell. Conversely, stomatal closure results from efflux of solutes to the apoplast, which drives osmotic water loss and the decrease of guard-cell turgor pressure. Passive fluxes of K^+ down an electrochemical gradient, through the plasma membrane of guard cells, are mediated by two types of voltage-gated K-selective ion channels: inward rectifier K channels, which are activated upon hyperpolarization of the plasma membrane (K_H channels) and serve as the main conduit for K^+ influx, and outward rectifier K channels, which are activated by depolarization (K_D channels) and allow the release of internal K^+ (Schroeder et al., 1987; Schroeder, 1988).

Agents affecting the activity of K channels affect stomatal movements. For example, an increase of external

---

and/or cytosolic Ca^{2+} concentrations inhibits K_H channels (Schroeder and Hagiwara, 1989; Busch et al., 1990; Fairley-Grenot and Assmann, 1992) and inhibits stomatal opening (De Silva et al., 1985). Additionally, this $[Ca^{2+}]$ increase leads to indirect opening of K_D channels (via the opening of Cl channels and depolarization; Schroeder and Hagiwara, 1989) and promotes stomatal closure (Schwartz, 1985; Gilroy et al., 1990; McAinsh et al., 1990). External Al^{3+}, which blocks K_H channels (Schroeder, 1988), prevents stomatal opening (Schnabl and Ziegler, 1975). It is therefore tempting to seek explanations for the effects of temperature on stomatal aperture at the level of K channels. However, in spite of the remarkable effects of temperature on stomatal aperture, there is no available information regarding its direct effect on the regulation of guard-cell ion fluxes, and only partial information exists concerning the temperature dependence of ion channel activity in any plant cell. The activation of K channels in whole *Arabidopsis thaliana* cultured cells (and whole vacuoles) was promoted by warming between 15 and 22°C (Colombo and Cerana, 1993). The activation of single mechanosensory Ca channels in onion epidermal cells was enhanced by lowering the temperature between 26 and 5°C (Ding and Pickard, 1993).

In view of these dissimilar results and in the hope of gaining insight into the mechanism underlying temperature regulation of stomatal aperture, we examined the effect of a wide range of temperature (13–36°C) on the separate properties of conductance and gating of plant K channels in the plasma membrane of guard-cell protoplasts isolated from *V. faba* leaves.

MATERIALS AND METHODS

Plant Material

Plants of *Vicia faba* were grown under controlled environmental conditions as described previously (Ilan et al., 1994). Growth temperature was kept at 22°C during the day and 17°C at night. Guard-cell protoplasts were isolated from young, fully expanded leaves of 3- to 4-week-old *V. faba* plants according to the procedure of Kruse et al. (1989). The average diameter of the spherical guard-cell protoplast was 16.6 ± 1.2 μm (mean ± SD, n = 122), and the calculated average cell surface was 865 ± 125 μm^2.

Temperature Control

During the electrophysiological measurements, the temperature of the protoplast suspension was controlled by heat conduction between the recording Plexiglas chamber holding the protoplasts and a silver plate beneath it. The silver plate was heated or cooled by two, mounted thermoelectric (Peltier) heat-pump modules on both sides of the chamber (built by Technical Video, Ltd., Woods Hole, MA). The temperature change was monitored directly by a thermistor dipped in the solution bathing the protoplasts. Measurements were started at least 10 min after the new temperature was reached.

Electrophysiology

We used the patch-clamp technique both in the whole-cell configuration and in excised outside-out membrane patches (Hamill et al., 1981). Experiments were performed in a voltage-clamp mode as described by Ilan et al. (1994), and we measured currents elicited by preprogrammed depolarizing and hyperpolarizing voltage pulses applied at 20- or 13-s intervals, respectively. All E_M values were corrected for liquid-junction potentials, measured using 3 M KCl-agar bridges, by −17 mV when the $[K^+]_o$ was 11 mM and by −8 mV when $[K^+]_o$ was 50 mM. Whole-cell K^+ currents were low-pass filtered and sampled according to the tested temperatures as follows: the corner frequency (−3 dB point) of the four-pole Bessel filter was, for the K_H channel currents, 100 Hz at 13°C, 200 Hz at 20°C, and 500 Hz at 28 and 36°C. K_D channel currents were filtered at 50 Hz at 13°C, at 100 Hz at 20°C, and at 200 Hz at the higher temperatures. In all of these cases, the sampling frequency was 2- to 3-fold higher than that of the filter used. Unitary K_H currents were filtered at 500 Hz and unitary K_D currents were filtered at 200 Hz. In the single-channel experiments, the sampling rate was 2 kHz.

Analysis

I_K values were obtained by subtracting the leak current (the instantaneous current at the beginning of the voltage pulses, Ilan et al., 1994) from the current measured at the end of the voltage pulses. We calculated G_K at various E_Ms, from the relation between I_K and E_M.

$$I_K = G_K \cdot (E_M - E_{rev}), \tag{1}$$

where E_{rev} is the reversal potential of the currents. The E_{rev}s of the two current types were determined from tail-current experiments (Hodgkin and Huxley, 1952). The linearity of the instantaneous whole-cell I_K-E_M relationships, as well as of the unitary i_s-E_M relationships, in the presence of 11 mM K^+ in the external solution (Ilan et al., 1994; and our unpublished data), justifies the use of Equation 1 for the calculation of G_K of both K_D and K_H channels. At all E_Ms, G_K reflects two factors:

$$G_K = G_{max} \cdot P_o, \tag{2}$$

where P_o is the voltage-dependent probability for a K channel to be open ("open probability"). At a voltage range at which P_o saturates at 1, G_K reaches its maximum, G_{max}, which in turn reflects two factors:

$$G_{max} = N \cdot \gamma_s, \tag{3a}$$

where N is the number of channels in the cell membrane available for activation by E_M and γ_s is the single-channel conductance. Furthermore,

$$N = N' \cdot f_a, \tag{3b}$$

where N' is the total number of channel molecules in the membrane, assumed to be constant in the time scale of the experiment, and f_a is the activatable fraction, which may vary in the course of the experiment depending on the prevailing conditions. Note that (a) both N' and f_a are

voltage independent and (b) changes in N reflect changes in f_a.

To extract G_{max} from steady-state G_K-E_M relationships, we replaced the voltage-dependent steady-state P_o with the simple Boltzman relationship:

$$G_K = G_{max}/(1 + e^{-zF \cdot (E_M - E_{1/2})/RT}), \qquad (4)$$

where R is the universal gas constant, F is the Faraday constant, and T is the absolute temperature. $E_{1/2}$ is the half-activation voltage, and z is the number of effective charges transferred upon the transition between the open and the closed states of the channel with the underlying assumption of an equilibrium between these two main states. It should be noted that this serves only as a first approximation, at least in the case of the K_D channels, which undergo transitions between one open state and at least two closed states (Schroeder, 1989; Fairley-Grenot and Assmann, 1993; Ilan et al., 1994).

Equation 4 was fitted to the individual G_K-E_M relationships of K_D channels, determined separately for each cell and at each temperature. Then, with the sign of the exponent inverted, Equation 4 was fitted also to G_{K_H}-E_M. For fitting we used the 386-Matlab program subroutine from Mathworks, Inc. (Natick, MA), implementing the Nelder-Meade simplex algorithm for error minimization, with equal weights assigned to all data points.

i_s amplitudes were determined from the inter-peak distances of the amplitude histograms of steady-state, single-channel current records at various E_M in outside-out patches (Ilan et al., 1994). γ_s was estimated from the slopes of the unitary i_s-E_M relationships. Ahrenius relationship was used to calculate the E_a of ion permeation in the K channels from the temperature dependence of γ_s:

$$\gamma_s = Ae^{-E_a/RT}, \qquad (5)$$

where A is an empirical constant (Hille, 1992). The above 386 Matlab subroutine was used to fit this equation to the mean γ_s versus temperature data of K_H and K_D channels, with the inverse of SD used as weights. The Q_{10} of conductance change was calculated from:

$$Q_{10} = e^{(E_a/R \cdot 10/T_m \cdot [T_m + 10])}, \qquad (6a)$$

where T_m is the midrange value of the temperature (in K). Alternatively, when using data of others for the sake of comparison, Q_{10} was calculated from the ratio between the conductances γ_{s1} and γ_{s2}, determined at the respective temperatures T_1 and T_2, according to:

$$Q_{10} = (\gamma_{s2}/\gamma_{s1})^{10/(T_2 - T_1) \cdot T_2 \cdot T_1/T_m \cdot (T_m + 10)}. \qquad (6b)$$

The mean number of available channels in a cell at each temperature, N_K, was calculated by averaging the ratio between the individual values of G_{max} and the mean value of γ_s:

$$N = G_{max}/\gamma_s. \qquad (7)$$

Single K_D channel currents were recorded at conditions identical with those of whole-cell K_D currents. The single-channel K_H experiments were done at higher $[K]_o$ than the

whole-cell experiments (50 mM; to increase signal-to-noise ratio of the unitary K_H currents). Therefore, to enable the calculation of N_{K_H}, we calculated first the expected γ_{s-K_H} values at $[K]_o = 11$ mM from the mean γ_{s-K_H} values at $[K]_o = 50$ mM at the different temperatures. We used the ratio of 2.2, determined at 20°C between γ_s at 50 mM $[K]_o$ and γ_s at 11 mM $[K]_o$ under the plausible assumption that this ratio is constant at all the temperatures, i.e. that the same temperature dependence holds for ion permeation at both $[K]_o$. Then we used these calculated γ_{s-K_H} values to calculate the N_{K_H} values by Equation 7.

Solutions

The bath solutions contained (in mM): 1 Ca^{2+}, 2 Mg^{2+}, 6 Cl^-, 10 glutamate, 10 Mes, pH 5.5, and 11 K^+ or 50 K^+ (in K_H single-channel experiments and a few whole-cell experiments). Final osmolarity was adjusted with mannitol to 480 mOsm kg^{-1}. The intracellular solution in the patch pipette contained (in mM): 100 glutamate, 105 K^+, 6 Mg^{2+}, 4 Cl^-, 4 ATP, 20 Hepes, pH 7.2, and mannitol, to final osmolarity of 520 mOsm kg^{-1}. The cytosolic Ca^{2+} concentration, $[Ca^{2+}]_i$, was buffered with (a) 0.2 mM BAPTA without added $CaCl_2$ or (b) in experiments with 50 mM $[K]_o$, with 2 mM BAPTA and 1 mM $CaCl_2$. In (b) the free $[Ca^{2+}]_i$, on the basis of the dissociation constant of BAPTA, in the presence of 1 mM $CaCl_2$, was ≥ 200 nM (Pethig et al., 1989), and in case (a), only the upper limit of free $[Ca^{2+}]_i$ would be 200 nM, assuming a total Ca^{2+} contamination in the solution of ≤ 100 μM. Most likely, however, the Ca^{2+} contamination and therefore the free $[Ca^{2+}]$ in these solutions were much lower.

RESULTS

Temperature Effects on Whole-Cell K^+ Currents

We recorded whole-cell K^+ currents through the K_H channels and through the K_D channels of guard-cell protoplasts during short-term exposures to different temperatures in the range between 13 and 36°C. Figure 1 illustrates the effects of low temperature (13°C) on these currents. Lowering the temperature from the control conditions at 20 to 13°C had a similar effect on both channel types: it decreased currents via K_H channels (Fig. 1, A and B) as well as those via K_D channels (Fig. 1, C and D). In contrast, high temperature (36°C) had an opposite effect on the magnitudes of the two current types, as shown in Figure 2. Raising the temperature from 20°C up to 36°C increased the K_H currents (Fig. 2, A and B) but drastically decreased the K_D currents (Fig. 2, C and D). All of the temperature effects on the steady-state K^+ currents amplitude were fully reversible (Figs. 1, B and D, and 2, B and D).

In addition to the temperature effects on the magnitude of the currents at steady-state, raising the temperature accelerated the kinetics of both currents. This can be seen in four typical examples shown in Figures 1, A and C, and 2, A and C, and is summarized as an effect on $t_{1/2}$ (the time for half-activation or half-deactivation) in Figure 3. The effect of cooling below 20°C on the kinetics was fully reversible (10 experiments with K_D channels and 12 experiments with
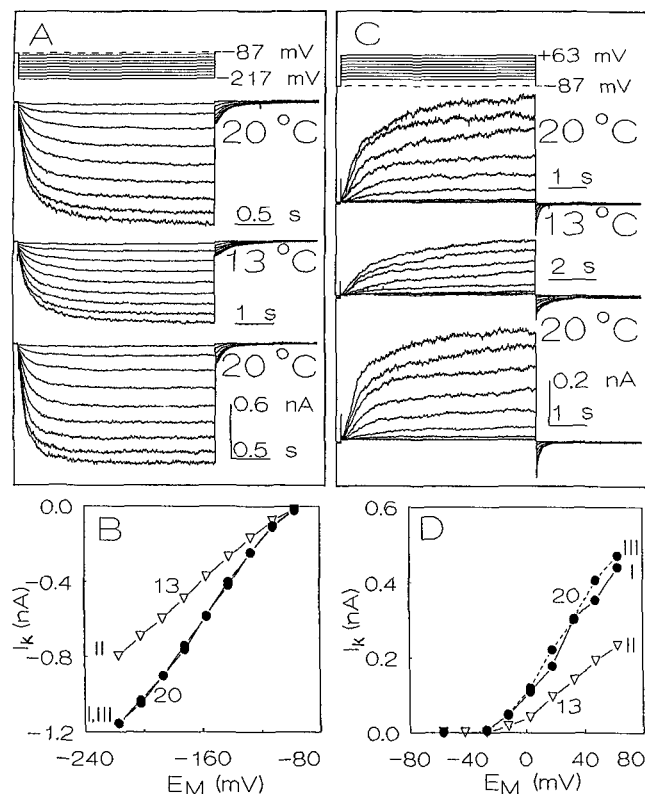
Figure 1. Low temperature (13°C) attenuates and retards K$^+$ currents. A and B, K$_H$ currents. C and D, K$_D$ currents (cell different from the one depicted in A and B). A and C, top, Protocol of voltage pulses (superimposed); bottom, time course of current relaxations (superimposed separately at each indicated temperature) elicited by the voltage pulses. Note the condensed time scale at 13°C. B and D, Steady-state current-voltage relationship of A and C, respectively, at 20°C (●) and 13°C (▽). The Roman numerals indicate the sequence of temperature changes.

K$_H$ channels; illustrated in Fig. 1). The effect of warming from 20 to 36°C was also completely reversible in the case of K$_H$ channels (14 experiments). However, in the case of K$_D$ channels (in the same cells with the reversibly affected K$_H$ channels), the reversibility was not always complete: after lowering the temperature from 36 to 20°C in about half of the experiments, the activation kinetics of the K$_D$ currents remained faster than before warming (in 6 of 10 cases; illustrated in Fig. 2C).

The aim of our analysis was to resolve the temperature dependence of the steady-state K$^+$ currents into the underlying components. Since the I_K is a function of the G_K and of the electrochemical potential of K$^+$, E_M-E_{rev} (Eq. 1), we examined initially the E_{rev} of both current types. The temperature effects on E_{rev} are summarized in Table I. Whole-cell E_{rev} became more negative with temperature, as did the calculated Nernst potential of K$^+$, E_K (see legend to Table I). Moreover, E_{rev} values of the K$_H$ currents became closer to E_K as the temperature increased, indicating that warming may have increased the whole-cell selectivity for K$^+$ at hyperpolarization potentials.

The tabulated E_{rev} values were then used to determine the G_K of the K$_H$ and K$_D$ channels (Eq. 1). Not surprisingly,

the effects of temperature on G_K, shown in Figure 4, A and B, parallel those already seen in the whole-cell currents. Whereas G_{K_H} increased monotonically with temperature and saturated at 28°C (Fig. 4A), G_{K_D} increased up to 20°C and decreased at higher temperatures (Fig. 4B).

To resolve which of the two factors, the voltage-independent G_{max} or the voltage-dependent P_o, making up the G_K (Eq. 2) are responsible for these effects of temperature, we examined each one separately. Temperature effects on G_{max} are shown in Figure 4, C and D. Upon heating from 13 to 20°C, G_{max-K_H} (Fig. 4C) and G_{max-K_D} (Fig. 4D) increased by 64 and 82%, respectively. When the temperature was elevated further from 20 to 28°C, G_{max-K_H} increased by 22%, but G_{max-K_D} decreased by 40%. A further temperature increase to 36°C had no significant effect on G_{max-K_H}, whereas it caused a dramatic decrease of G_{max-K_D} to 25% of the maximum.

Temperature effects on the P_o was limited to an effect on the $E_{1/2}$ (Eq. 4), as shown in Figure 4, E and F. The effective number of gating charges, z, was unaffected by temperature changes (see legend to Fig. 4, A and B). $E_{1/2}$ of the whole-cell K$_H$ channels shifted to significantly more nega-
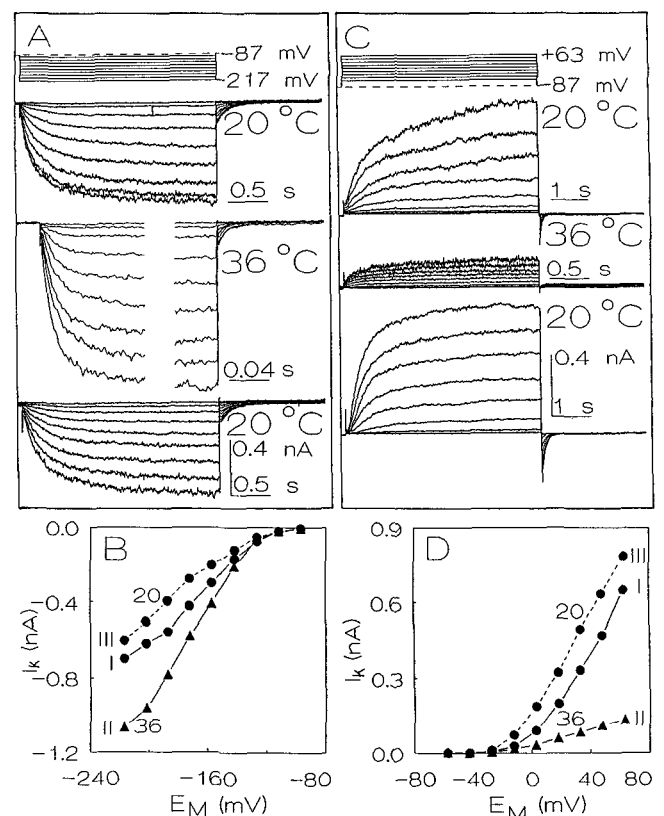

Figure 2. High temperature (36°C) accelerates K$^+$ currents, increases K$_H$ currents, but decreases K$_D$ currents. A and B, K$_H$ currents. C and D, K$_D$ currents (cell different from the one depicted in A and B). A and C, top, Protocol of voltage pulses; bottom, time course of current relaxations. Note the expanded time scale at 36°C, (and the gaps in traces, for presentation purpose only, of currents evoked by 1-s pulses). B and D, Steady-state current-voltage relationship of A and C, respectively, at 20°C (●) and 36°C (▲). The Roman numerals indicate the sequence of temperature changes.
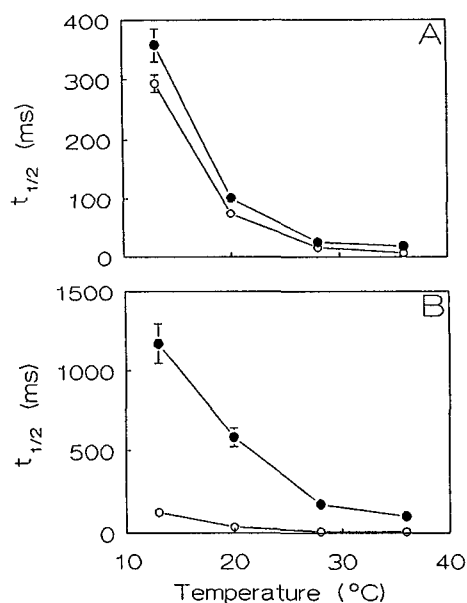
Figure 3. Temperature increase accelerates K channels kinetics. A, Mean (±SE) $t_{1/2}$ of activation at −217 mV (●) and deactivation at −87 mV (○) of the K_H channel currents. Averages from 6, 19, 4, and 9 cells at 13, 20, 28, and 36°C, respectively. B, Average (±SE) $t_{1/2}$ of activation at 78 mV (●) and deactivation at −87 mV (○) of the K_D channel currents. n = 4, 18, 4, and 10 at 13, 20, 28, and 36°C, respectively. Where not seen, SE bars were smaller than the symbol size.

tive potentials when the temperature was increased between 20 and 28°C (Fig. 4E), whereas $E_{1/2}$ of the K_D channels shifted to negative potentials only between 13 and 20°C and to more depolarized potentials with a temperature increase between 28 and 36°C (Fig. 4F).

Temperature Effects on Single K_H Channels

Since G_{max} depends, in turn, on N and on γ_s (Eq. 3a), an effect on either one of them could underlie the effect on G_{max}. Therefore, we directly examined the temperature effects on γ_s in outside-out patches. We identified the single K_H channels by (a) their voltage dependence: they were activated by hyperpolarization and deactivated upon the return to a more depolarized potential, (b) their selectivity to K$^+$: the E_{rev} of the unitary currents was the closest to the calculated Nernst potential of K$^+$ (the Nernst potentials of the three other permeant ions in the solutions, Ca^{2+}, H$^+$ and Cl$^-$ were, respectively, ≥200, +100, and −10 mV), and (c) their unitary conductance: γ_{s-K_H} was approximately 5 pS at 20°C with 11 mM external K$^+$ (N. Ilan, N. Moran, and A. Schwartz, unpublished data), consistent with the findings of Schroeder et al. (1987) and Schroeder and Hagiwara (1989). Since γ_{s-K_H} was relatively low, to increase the signal-to-noise ratio in the K_H single-channel experiments, external K$^+$ concentration was changed to 50 mM. γ_{s-K_H} at 20°C with 50 mM [K$^+$]$_o$ was 11 pS, consistent with the values of 14 to 20 pS determined in symmetrical 105 mM K$^+$ (Schroeder et al., 1987; Schroeder and Hedrich, 1989; see, however, Wu and Assmann, 1994).

The unitary conductance of the K_H channel increased with temperature as shown in Figure 5. The average γ_{s-K_H} values with 50 mM external K$^+$ were 7, 11 and 14 pS at 13, 20, and 28°C, respectively (Fig. 5, B and C). This temperature dependence may be interpreted as reflecting the energy of activation of K$^+$ permeation within the K_H channel (Eq. 5), amounting to 8.3 kcal/mol (35 kJ/mol) and equivalent to Q_{10} of 1.6 (Eq. 6a; reviewed by Hille, 1992).

Having determined γ_{s-K_H} (Fig. 5), we calculated the number of K_H channels available for activation by hyperpolarization in each cell at each temperature (Eq. 7). Temperature changes did not affect significantly the mean number of available K_H channels, N_{K_H}, which ranged between about 1200 channels per cell at 13 and 20°C to about 1050 channels per cell at 28°C (Fig. 6).

Temperature Effects on Single K_D Channels

As in the former case, we identified the single K_D channels as depolarization-activated K channels by several criteria: (a) their dependence on voltage: depolarization recruited K_D channel openings, and steps from depolarized potentials to negative potentials caused closing of K_D channels. In addition, at steady state the average number of open channels was significantly higher at 23 to 43 mV than at −17 to 3 mV (data not shown). (b) Their unitary conductance: γ_s =11 ± 0.3 pS at 20°C, identical with our former determination of 10 ± 1 pS (Ilan et al., 1994) and consistent with two other separate determinations: 25 pS with [K$^+$]$_i$/[K$^+$]$_o$ = 175/11 mM (Schroeder et al., 1987) and 15 pS with [K$^+$]$_i$/[K$^+$]$_o$ = 200/50 mM (Hosoi et al., 1988). (c) Their selectivity to K$^+$: at 20°C, the E_{rev} of the unitary currents was −52 ± 2 mV, whereas E_K was −53 mV. Furthermore, increasing [K$^+$]$_o$ to 50 mM shifted the calculated E_K by +36 mV and the E_{rev} of the unitary currents by +29 mV (not shown). Figure 7 shows the temperature effects on the conductance and the E_{rev} of the single K_D

Table I. Temperature effect on E_{rev} in whole cells

Values of the E_{rev} of whole-cell K$^+$ currents, determined by the "tail-current method" (Hodgkin and Huxley, 1952; see also Ilan et al., 1994), and the equilibrium potential of K$^+$, E_K, calculated from the Nernst equation:

$$E_K = - RT/F \ ln(a_{K_i}/a_{K_o})$$

a_{K_i} and a_{K_o} are the internal and external activities of K$^+$, respectively, calculated from K$^+$ concentrations using coefficients from appendix No. 8.9 from Robinson and Stokes (1965). K_H and K_D denote the current types. We were unable to determine E_{rev-K_D} at 28 and 36°C because of the small size of the tail currents (e.g. Fig. 2C). Therefore, we extrapolated these values (marked by *) from the E_{rev-K_D} value at 20°C using the theoretical slope of −1 mV/7°C. Numbers in parentheses are numbers of determinations.

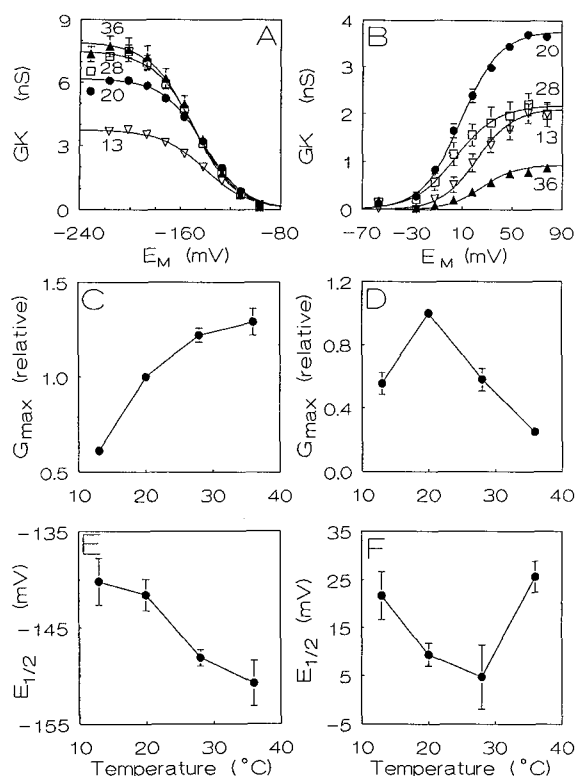| Temperature	E_{rev-K_H}	E_{rev-K_D}	Nernst E_K
°C	mV ± SE	mV ± SE	mV
13	−45 ± 0.4 (6)	−40.7 ± 1.2 (3)	−52
20	−49 ± 0.5 (20)	−42 ± 0.5 (16)	−53
28	−52 ± 0.9 (4)	−43*	−54
36	−55 ± 1.7 (7)	−44*	−56

Figure 4. Temperature dependence of G_{K_H} and G_{K_D}. A, Mean ($\pm$SE) steady-state conductance of K_H channels (G_{K_H}) versus E_M at the indicated temperatures: 13°C (∇, $n = 6$), 20°C ($\bullet$, $n = 18$), 28°C ($\square$, $n = 4$), and 36°C ($\blacktriangle$, $n = 8$). To minimize variability among cells, prior to averaging, G_{K_H} values at all temperatures were normalized to the asymptotic G_{max-K_H} at 20°C for the same cell. The mean ($\pm$SE) normalized G_{K_H} values were rescaled back to absolute values using the average G_{max-K_H} at 20°C of 6.2 $\pm$ 1.4 nS ($n = 17$). Where not seen, SE bars were smaller than symbol size. Lines, Calculated from the Boltzmann relationship (Eq. 4 with exponent sign inverted) using the following averaged best-fit parameters from the individual fits: G_{max-K_H} (rescaled, in nS), $E_{1/2-K_H}$ (in mV), and z_{K_H} respectively: 3.8, -140, 1.4 at 13°C; 6.2, -142, 1.5 at 20°C; 7.5, -148, 1.5 at 28°C and 7.9, -151, 1.5 at 36°C. B, Average (SE) chord conductance of K_D channels (G_{K_D}) versus E_M at the indicated temperatures: 13°C (∇, $n = 4$), 20°C ($\bullet$, $n = 18$), 28°C ($\square$, $n = 4$), and 36°C ($\blacktriangle$, $n = 10$). The average ($\pm$SD) G_{max-K_D} at 20°C, used for the rescaling of the mean normalized G_{K_D} values back to absolute values, was 3.8 $\pm$ 1.2 nS ($n = 18$). Lines, Calculated from Equation 4, using the averaged best-fit parameters: G_{max-K_D} (rescaled, in nS), $E_{1/2-K_D}$ (in mV), and z_{K_D}, respectively: 2, 22, 1.8 at 13°C; 3.8, 9, 1.6 at 20°C; 2.2, 5, 1.5 at 28°C, and 0.9, 26, 1.9 at 36°C. C and D, Temperature dependence of the maximum (voltage-independent) conductance, G_{max-K_H} and G_{max-K_D}, normalized to the corresponding G_{max} at 20°C. From the same data as A and B, respectively. E, Temperature dependence of the half-activation voltage, $E_{1/2-K_H}$, from the same data as those of A. The mean ($\pm$SE) values of $E_{1/2-K_H}$ were -140 ± 2.4, -142 ± 1.6, -148 ± 0.9, and -151 ± 2.4 at 13, 20, 28, and 36°C, respectively. The difference between $E_{1/2-K_H}$ at 20 and 28°C was significant with $P < 0.01$. F, Temperature dependence of the half-activation voltage, $E_{1/2-K_D}$, from the same data as those of B. The mean ($\pm$SE) values of $E_{1/2-K_D}$ were 21.7 $\pm$ 5, 9.3 $\pm$ 2.4, 4.7 $\pm$ 6.6, and 25.7 $\pm$ 3.3 at 13, 20, 28, and 36°C, respectively. The difference between $E_{1/2-K_D}$ at 13 and 20°C was significant with $P < 0.05$, and the difference between 28 and 36°C was significant with $P < 0.005$ (two-sided t test).

channels. The extrapolated values of E_{rev} of the single K_D channel currents (ranging between -48 and -52 mV) were close to the calculated E_K (Table I). We did not observe much change with temperature, probably because of some data scatter (Fig. 7B). Interestingly, at 13 and 20°C, these E_{rev} values were approximately 10 mV more hyperpolarized than those determined in the whole-cell experiments (Table I) and those determined previously in seven single-channel experiments at 20°C (-42 mV; Ilan et al., 1994). Like the shifted voltage dependence of the gating properties of single K_D channels in outside-out patches (Ilan et al., 1994), this apparently wider range of E_{rev} values of the unitary currents might be due to patch excision (Trautmann and Siegelbaum, 1983; Covarrubias and Steinbach, 1990). We based our further analyses on the assumption that the K_D unitary currents represent the whole-cell outward currents.

The γ_s of the K_D channel increased with temperature. The average γ_{s-K_D} were 8, 11, and 15 pS at 13, 20, and 28°C, respectively (Fig. 7, B and C). This temperature depen-
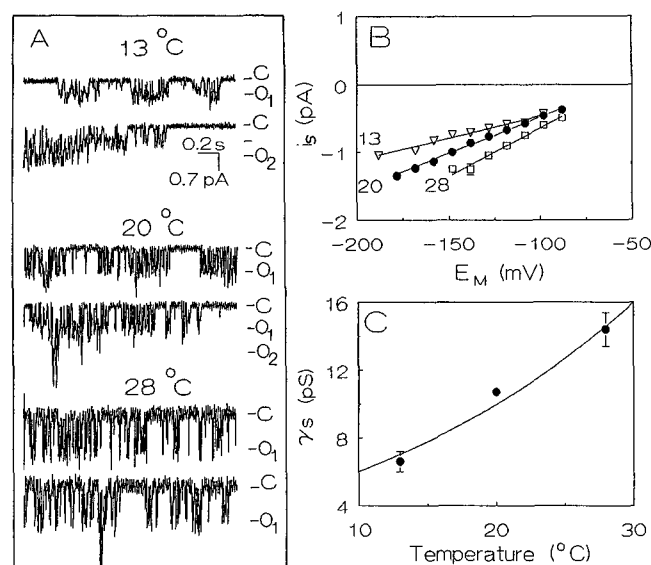

Figure 5. Temperature effects on single K_H channels. A, Sample traces of single-channel current at -128 mV from one outside-out patch with $[K^+]_o = 50$ mM at the indicated temperatures. Downward deflections indicate channel opening and inward current. C, O_1 and O_2 indicate levels of current with all channels closed or with one or two channels open, respectively. B, Unitary current-voltage (i_s-E_M) relationships at the following temperatures: ∇, 13°C; $\bullet$, 20°C; $\square$, 28°C. Symbols, Average ($\pm$SE) i_s from 2–3, 5–13, and 4–7 patches, respectively. Where not seen, SE was smaller than the symbol size. Lines, Linear regression fit to the pooled data prior to averaging. The unitary K_H channel conductance, γ_{s-K_H}, was 6.6 $\pm$ 0.6 pS at 13°C, 10.7 $\pm$ 0.3 pS at 20°C, and 14.4 $\pm$ 1 pS at 28°C. The E_{rev} of these currents cannot be determined by linear extrapolation because of rectification as observed in instantaneous whole-cell currents (not shown). We attribute this rectification to the coincidentally altered $[Ca^{2+}]_i$ (see "Solutions"). C, Temperature dependence of γ_{s-K_H}. Symbols represent the slopes of the i_s-E_M relationships ($\pm$SE) of B. Line, The fit of Ahrenius relationship (Eq. 5) to the data points. The best fit values were: $E_a = 8$ kcal or 35 kJ and A, 1.6 $\times$ 10^7 pS.
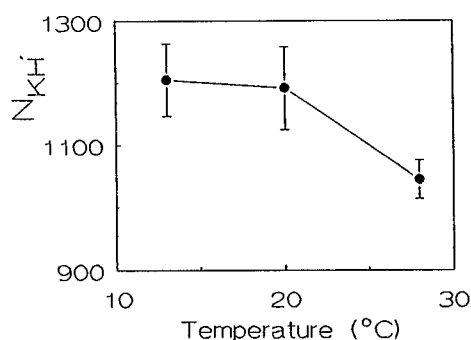
Figure 6. N_{K_H} is not affected by temperature. The mean ($\pm$SE) whole-cell numbers of available K_H channels (N_{K_H}) calculated from the mean values of $G_{max-K_H}/\gamma_{s-K_H}$ (see text for details) were: 1205 $\pm$ 59, 1192 $\pm$ 67, and 1045 $\pm$ 31 at 13, 20, and 28°C, respectively. The differences between any two means were not significant (two-sided t test; $P > 0.05$).

dence corresponds to E_a of 6.6 kcal/mol (28 kJ/mol) and Q_{10} of 1.5 (Eq. 6a). As before, we calculated the number of available K_D channels in each cell at the different temperatures. As shown in Figure 8, the mean N_{K_D} values in each case were significantly different: N_{K_D} increased from about 260 at 13°C to about 360 at 20°C and decreased markedly to about 170 channels per cell at 28°C.

DISCUSSION

The promotion in guard cells of K^+ current amplitudes by increasing temperature between 13 and 20°C, shown in Figure 1, may be compared to that reported for K^+ currents in the plasma membrane of Arabidopsis cultured cells (Colombo and Cerana, 1993). In both preparations, a temperature increase between 13 and 20°C increased the amplitudes of whole-cell currents through both the K_H and the K_D channels and accelerated the time constants of activation of the K_H channels. Contrary to our finding, however (see Figs. 1C and 3B), in Arabidopsis raising the temperature did not affect the kinetics of the K_D channels. In our study, we extended the examination of temperature effects on K_D and K_H channels to higher temperatures, focusing separately on the steady-state properties of the open channels and on their gating. Furthermore, we resolved the effects of temperature on the conductance at the level of single channels.

Temperature Effects on Ion Permeation via the Open K Channels

The effects of temperature on the passage of K^+ ions through the open channels, described in this report, were generally predictable from the temperature effects on electrodiffusion in water. The γ_s of both channel types increased almost linearly with temperature (Figs. 5C and 7C). The calculated Q_{10} values of this temperature dependence (Eq. 6a) were 1.6 and 1.5 for the K_H and K_D channels, respectively. Ding and Pickard (1993) reported a 1.3-fold increase of γ_s of mechanosensory Ca channels at a temperature range of 11 to 25°C, equivalent to Q_{10} of 1.2 (Eq. 6b).

Similar values of Q_{10} of γ_s are rather common in various channels in animal cells. For example, in K channels in T lymphocytes Q_{10} was 1.2 (Pahapill and Schlichter, 1990); in K channels in cardiac sarcoplasmic reticulum, it was 1.2 (Shen et al., 1993); and in cardiac inward rectifier-ATP-dependent K channels, the Q_{10} was 1.4 (McLarnon et al., 1993). In Na channels of the squid axon Q_{10} was 1.5 (Correa et al., 1991), in the cation-selective acetylcholine-receptor channel in cultured BC3H-1 cells Q_{10} was 1.4 (Dilger et al., 1991), but it was approximately 2.0 in the garter snake end plate acetylcholine-receptor channels (Hoffmann and Dionne, 1983). For comparison, the Q_{10} of the increase of the limiting equivalent conductivity of K^+ in water is 1.2 (calculated by eq. 6b from Robinson and Stokes, 1965; appendix 6.2). Thus, the passage of K^+ in both K_D and K_H channel types of Vicia guard cells resembles diffusion in an aqueous medium.

The increase of γ_{s-K_H} with the temperature increase (Fig. 5C) could account wholly for the increase in G_{max-K_H} (Fig. 4C); both of them increased 2-fold with a temperature increase between 13 and 28°C. In contrast, the increase in γ_{s-K_D} with temperature accounts for only about half of the increase in whole-cell G_{max-K_D} in the range of 13 and 20°C
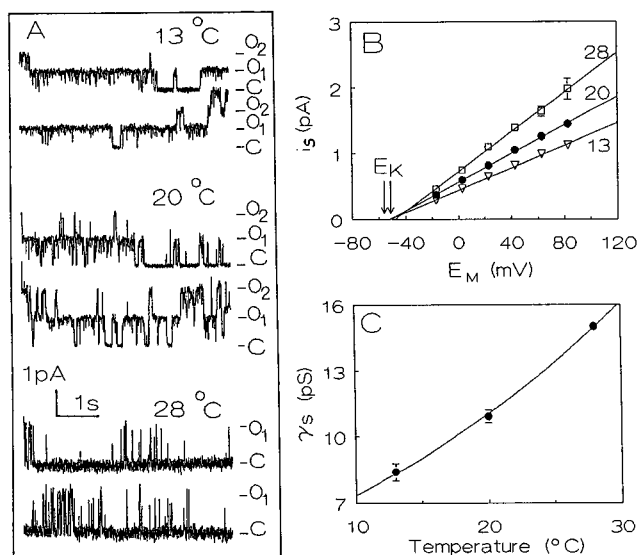

Figure 7. Temperature effects on single K_D channels. A, Sample traces of single-channel currents at 23 mV from one outside-out patch at the indicated temperatures. Upward deflections indicate open channels and outward current. C, O_1 and O_2 indicate, respectively, levels of current with all channels closed or with one or two channels open. B, Unitary current-voltage (i_s-E_M) relationships of K_D channels at the indicated temperatures: ∇, 13°C; ●, 20°C; □, 28°C. Data represent average ($\pm$SE) i_s from 4–7, 14–19, 4–5 patches, respectively. Where not seen, SE was smaller than the symbol size. Lines, Linear regression fit to the pooled data prior to averaging. The γ_s was 8.4 $\pm$ 0.4 pS at 13°C, 10.9 $\pm$ 0.3 pS at 20°C, and 15 $\pm$ 0.1 pS at 28°C, and the respective E_{rev} were -52 ± 3 mV, -52 ± 2 mV, and -48 ± 3 mV. The arrows mark the corresponding range of the calculated E_K. C, Temperature dependence of γ_{s-K_D}. Symbols represent the slopes of the i_s-E_M relationships ($\pm$SE) of B. Line, The fit of Ahrenius relationship (Eq. 5) to the data points, with the best fit values: $E_a = 6.7$ kcal or 28 kJ and $A = 1.07 \times 10^6$ pS.
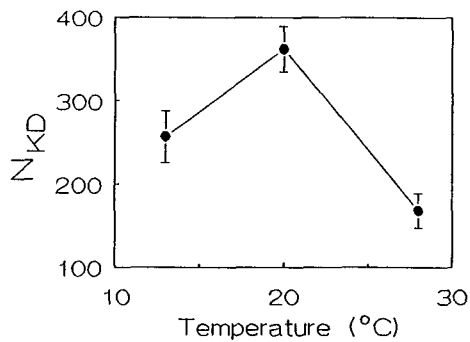
Figure 8. Significant temperature effect on N_{K_D}. The average ($\pm$ SE) whole-cell numbers of available K_D channels (N_{K_D}), calculated from the ratio $G_{max-K_D}/\gamma_{s-K_D}$, as in Figure 6, were 257 $\pm$ 31 at 13°C, 362 $\pm$ 27 at 20°C, and 168 $\pm$ 21 at 28°C. The differences between N_{K_D} values at 20°C and the other temperatures were significant with $P <$ 0.02 (two-sided t test).

(Figs. 4D and 7), and not at all for the decrease of G_{max-K_D} above 20°C.

Temperature Effects on K Channels Gating

The temperature effects mentioned so far affect the open channel, but the change of current kinetics with temperature (Figs. 1–3) indicates clearly additional effects of temperature on channel gating. Further studies are required to resolve these effects of temperature into separate effects on the transitions of the channels between their open and their closed conformations. Here, assuming an equilibrium between two major states, "open" and "closed," we will note only the effects of temperature on the steady-state properties of gating: on the voltage dependence of the P_o and on the voltage-independent N (Eq. 3b). As noted above, N reflects the fraction, f_a, of channels that will respond to any change in the electrical field in the membrane. The size of this fraction constitutes a manifestation of voltage-independent modulation of channel gating and it may be affected by temperature through the state of membrane matrix (e.g. degree of fluidity) or through the direct or indirect interactions of membrane lipids or enzymes with the channel macromolecule, leading to phosphorylation, methylation, their reversal, etc. An indirect modification may include, for example, an effect of temperature on putative cytoskeletal elements attached to the K_D channel (channel modulation by cytoskeletal elements in animal cells were analyzed in a number of recent publications: for example, Froehner, 1991; Lecar and Morris, 1993; Rosenmund and Westbrook, 1993).

N_{K_H}, the calculated number of available K_H channels, was not affected significantly by the temperature changes (Fig. 6). This may serve as an indication that the availability of K_H channels was largely unaffected by the temperature change in this range. In contrast, according to our interpretation, the increased availability of K_D channels, N_{K_D}, between 13 and 20°C (Fig. 8) is responsible for about half of the increase in G_{max-K_D}. Furthermore, we interpret the disparity between the marked decrease of G_{max-K_D} despite the continued increase in γ_{s-K_D}, at the temperature range 20 to

28°C, as a drastic decrease of N_{K_D} and we believe that this underlies also the further decrease of G_{max-K_D} above 28°C. A reversible decline of channel responsivity (to activation by mechanical stretch) with temperature increase has been observed also in mechanosensory Ca channels in onion epidermis protoplasts, albeit in a lower temperature range of between 6 and 26°C (Ding and Pickard, 1993). The different effect of heating on the available number of *Vicia* K_H and K_D channels indicates that temperature effects are localized, unlike a general change in membrane fluidity. The decrease of availability of K_D channels (Fig. 8) may reflect immobilization, or "locking" (reversible upon cooling), of the channel gates at some "superclosed" conformation. Further experiments are required to examine these hypotheses.

In addition to the effect of temperature on the voltage-independent N, temperature affects also the voltage dependence of the P_o. It is interesting to note that, within the framework of the simplified model of open↔closed equilibrium, this is not due to any change in the gating subunits themselves (once they are "unlocked"), since the effective number of gating charges, z, was unaffected by temperature changes (Fig. 4, A and B). Rather, the shifts of $E_{1/2}$ (i.e. of the P_o-E_M curve) reflect an altered electrical field in the membrane. The negative shift of $E_{1/2}$ of the K_H channels (by -7 mV) with the increase of temperature between 20 and 28°C (Fig. 4E) indicates that a larger hyperpolarization would be required to attain the same fraction of K_H channels open at steady state. A similar negative shift of $E_{1/2}$ (by -12 mV), albeit at the lower range of 13 to 20°C, occurs also in the P_o-E_M curve of the K_D channel (Fig. 4F). Here, however, it indicates that a smaller depolarization is required at the higher temperatures to open the same fraction of K_D channels. A converse effect is observed when the temperature is elevated further, between 28 and 36°C: $E_{1/2}$ of the K_D channels shifts to more depolarized potentials (by 21 mV) increasing the depolarization needed to activate the same fraction of K_D channels. Since $E_{1/2}$ of the K_H and K_D channels was not affected similarly by temperature, the change in electrical field should also be localized to the vicinity of each of the channels.

In summary, at all temperatures above 13°C, the overall K_H conductance increases because of the increase of the conductance of each open K_H channel, in spite of the relatively minor opposite effect of the reduced voltage-dependent P_o. Up to 20°C, the whole-cell K_D conductance increases because of the combined increase of unitary conductance availability and P_o. At temperatures above 20°C, the overall K_D conductance decreases drastically because of the combined effect of (a) the decreased voltage-independent availability of K_D channels and (b) decreased voltage-dependent P_o. These two effects override the relatively minor increase of the unitary K_D channel conductance.

Physiological Significance

The opposite effect of temperature elevation above 20°C on the steady-state whole-cell conductance of the K_H and

K_D channels presented in this paper is consistent with the stomata response to heat. The tendency of stomata to open at a higher temperature (Rogers et al., 1979, 1981) probably reflects an increase in H^+ pump activity (Du Pont, 1989), combined with enhanced whole-cell conductance of K_H channels, conditions that favor K^+ influx. The reduction of stomatal closure in the dark at the high temperature (Mansfield, 1965) can be explained by the pronounced decrease in whole-cell K_D conductance, resulting in reduced K^+ loss from the guard cells. Reduced K^+ exit diminishes the efflux of anions by preventing the dissipation of the built-up charge imbalance and thus retards the turgor decrease of the guard cells.

ACKNOWLEDGMENTS

LITERATURE CITED

Assmann SM (1993) Signal transduction in guard cells. Annu Rev Cell Biol 9: 345–375

Berry J, Bjorkman O (1980) Photosynthetic response and adaptation to temperature in higher plants. Annu Rev Plant Physiol 31: 491–543

Busch H, Hedrich R, Raschke K (1990) External calcium blocks inward rectifier potassium channels in guard cell protoplasts in a voltage and concentration dependent manner (abstract No. 96). Plant Physiol 93: S-17

Colombo R, Cerana R (1993) Effect of temperature on plasma membrane and tonoplast ion channels in Arabidopsis thaliana. Physiol Plant 87: 118–124

Correa AN, Latorre R, Bezanilla F (1991) Ion permeation in normal and batrachotoxin-modified Na^+ channels in the squid giant-axon. J Gen Physiol 97: 605–625

Covarrubias M, Steinbach JH (1990) Excision of membrane patches reduces the mean open time of nicotinic acetylcholine receptors. Pflugers Arch 416: 385–392

De Silva DLR, Cox RC, Hetherington AM, Mansfield TA (1985) Suggested involvement of calcium and calmodulin in the responses of stomata to abscisic acid. New Phytol 101: 555–563

Dilger JP, Brett RS, Poppers DM, Liu Y (1991) The temperature dependence of some kinetic and conductance properties of acetylcholine receptor channels. Biochim Biophys Acta 1063: 253–258

Ding JP, Picard BG (1993) Modulation of mechanosensitive calcium-selective cation channels by temperature. Plant J 3: 713–720

Du Pont FM (1989) Effect of temperature on the plasma membrane and tonoplast ATPases of barley roots. Plant Physiol 89: 1401–1412

Fairley-Grenot KA, Assmann SM (1992) Permeation of Ca^{2+} through K^+ channels in the plasma membrane of Vicia faba guard cells. J Membr Biol 128: 103–113

Fairley-Grenot KA, Assmann SM (1993) Comparison of K^+-channel activation and deactivation in guard cells from dicotyledon (Vicia faba L.) and a graminaceous monocotyledon (Zea mays). Planta 189: 410–419

Froehner S (1991) The submembrane machinery for nicotinic acetylcholine receptor clustering. J Cell Biol 114: 1–7

Gates DM (1968) Transpiration and leaf temperature. Annu Rev Plant Physiol 19: 211–238

Gilroy S, Read Nd, Trewavas AJ (1990) Elevation of cytoplasmic Ca^{2+} by caged calcium or caged inositol triphosphate initiates stomatal closure. Nature 346: 769–771

Hamill OP, Marty A, Neher E, Sakman B, Sigworth FJ (1981) Improved patch-clamp techniques for high resolution current recording from cells and cell-free membrane patches. Pflugers Arch 391: 85–100

Hille B (1992) Ionic Channels of Excitable Membranes. Sinauer Associates, Sunderland, MA

Hodgkin AI, Huxley AF (1952) A quantitative description of membrane current and its application to conduction and excitation in nerve. J Physiol 117: 500–544

Hoffmann HM, Dionne VE (1983) Temperature dependence of ion permeation at the endplate channel. J Gen Physiol 81: 687–703

Ilan N, Schwartz A, Moran N (1994) External pH effects on the depolarization-activated K channels in guard cell protoplasts of Vicia faba. J Gen Physiol 103: 807–831

Kappen L, Schultz G, Vanselow R (1994) Direct observation of stomatal movements. In ED Schulze, MM Caldwell, eds, Ecophysiology of Photosynthesis. Springer-Verlag, New York, pp 231–246

Kebede H, Johanson RC, Ferris DM (1989) Photosynthetic response of Eragrostis tef to temperature. Physiol Plant 77: 262–266

Kruse T, Tallman G, Zeiger E (1989) Isolation of guard cell protoplasts from mechanically prepared epidermis of Vicia faba leaves. Plant Physiol 90: 1382–1386

Lecar H, Morris CE (1993) Biophysics of mechanotransduction. In GM Rubanyi, ed, Mechanoreception by the Vascular Wall. Futura Publishing, Mount Kisco, NY

Mansfield TA (1965) Stomatal opening in high temperature in darkness. J Exp Bot 16: 721–731

Mansfield TA, Hetherington AM, Atkinson JC (1990) Some current aspects of stomatal physiology. Annu Rev Plant Physiol Mol Biol 41: 55–75

McAinsh MR, Brownlee C, Hetheringon AM (1990) Abscisic acid-induced elevation of guard cell cytosolic Ca^{2+} precedes stomatal closure. Nature 343: 186–188

McLarnon JG, Hamman BN, Tibbits GF (1993) Temperature dependence of unitary properties of an ATP-dependent potassium channel in cardiac myocytes. Biophys J 65: 2013–2020

Pahapill PA, Schlichter L (1990) Modulation of potassium channels in human T lymphocytes: effects of temperature. J Physiol 422: 103–126

Pethig R, Kuhn M, Payne R, Adler E, Chen T-H, Jaffe LF (1989) On the dissociation constants of BAPTA-type calicum buffers. Cell Calcium 10: 491–498

Radin JW, Lu Z, Pichard RG, Zeiger E (1994) Genetic variability for stomatal conductance in Pima cotton and its relation to improvement of heat adaptation. Proc Natl Acad Sci USA 91: 7217–7221

Raschke K (1970) Temperature dependence of CO_2 assimilation and stomatal aperture in leaf sections of Zea mays. Planta 91: 336–363

Raschke K (1975) Stomatal action. Annu Rev Plant Physiol 26: 309–340

Robinson RA, Stokes RH (1965) Electrolyte Solutions. Butterworths, London

Rogers CA, Powell RD, Sharpe PJH (1979) Relationship of temperature to stomatal aperture and potassium accumulation in guard cells of Vicia faba. Plant Physiol 63: 388–391

Rogers CA, Sharpe PJH, Powell RD (1981) High temperature disruption of guard cells of Vicia faba. Effect on stomatal aperture. Plant Physiol 67: 193–196

Rosenmund C, Westbrook GL (1993) Calcium-induced actin depolarization reduces NMDA channel activity. Neuron 10: 805–814

Schnabl H, Ziegler H (1975) Uber die Wirkung von Aluminiumionen auf die Stomatabewegung von Vicia faba Epidermen. Z Pflanzenphysiol 74: 394–403

Schroeder JI (1988) K^+ transport properties of K^+ channels in the plasma membrane of Vicia faba guard cells. J Gen Physiol 92: 667–683

Schroeder JI (1989) Quantitative analysis of outward rectifying K^+ channel currents in guard cell protoplasts from Vicia faba. J Membr Biol 107: 229–235

Schroeder JI, Hagiwara S (1989) Cytosolic calcium regulates ion channels in the plasma membrane of *Vicia faba* guard cells. Nature **338:** 427–430

Schroeder JI, Hedrich R (1989) Involvement of ion channels and active transport in osmoregulation and signaling of higher plant cells. Trends Biochem Sci USA **87:** 9305–9309

Schroeder JI, Raschke K, Neher E (1987) Voltage dependence of K^+ channels in guard cell protoplasts. Proc Natl Acad Sci USA **84:** 4108–4112

Schwartz A (1985) Role of Ca^{2+} and EGTA on stomatal movements in *Commelina communis* L. Plant Physiol **79:** 1003–1005

Shen WK, Rasmusson RL, Liu Q-Y, Crews AL, Strauss HC (1993) Voltage and temperature dependence of single K^+ channels isolated from canine cardiac sarcoplasmic reticulum. Biophys J **65:** 747–754

Sheriff DW (1979) Stomatal aperture and the sensing of the environment by guard cells. Plant Cell Environ **2:** 15–22

Trautmann A, Siegelbaum SA (1983) The influence of membrane isolation on single acetylcholine-channel current in rat myotubes. *In* B Sakmann, E Neher, eds, Single-Channel Recording. Plenum Press, New York, pp 473–480

Wu WH, Assmann SM (1994) A membrane-delimited pathway of G-protein regulation of the guard-cell inward K^+ channel. Proc Natl Acad Sci USA **91:** 6310–6319

Zeiger E (1983) The biology of stomatal guard cells. Annu Rev Plant Physiol **34:** 441–475